

## Site-specific analysis of N-linked oligosaccharides of recombinant lysosomal arylsulfatase A produced in different cell lines

Stephan Schröder, Frank Matthes, Pia Hyden, Claes Andersson, Jens Fogh, Sven Müller-Loennies, Thomas Braulke, Volkmar Gieselmann, Ulrich Matzner

### Angaben zur Veröffentlichung / Publication details:

Schröder, Stephan, Frank Matthes, Pia Hyden, Claes Andersson, Jens Fogh, Sven Müller-Loennies, Thomas Braulke, Volkmar Gieselmann, and Ulrich Matzner. 2010. "Site-specific analysis of N-linked oligosaccharides of recombinant lysosomal arylsulfatase A produced in different cell lines." *Glycobiology* 20 (2): 248-59. <https://doi.org/10.1093/glycob/cwp171>.

### Nutzungsbedingungen / Terms of use:

licgercopyright

Dieses Dokument wird unter folgenden Bedingungen zur Verfügung gestellt: / This document is made available under these conditions:

**Deutsches Urheberrecht**

Weitere Informationen finden Sie unter: / For more information see:

<https://www.uni-augsburg.de/de/organisation/bibliothek/publizieren-zitieren-archivieren/publiz/>



# Site-specific analysis of *N*-linked oligosaccharides of recombinant lysosomal arylsulfatase A produced in different cell lines

Stephan Schröder<sup>2</sup>, Frank Matthes<sup>2</sup>, Pia Hyden<sup>3</sup>, Claes Andersson<sup>3</sup>, Jens Fogh<sup>3</sup>, Sven Müller-Loennies<sup>4</sup>, Thomas Braulke<sup>5</sup>, Volkmar Gieselmann<sup>2</sup>, and Ulrich Matzner<sup>1,2</sup>

<sup>2</sup>Rheinische Friedrich-Wilhelms Universität, Institut für Biochemie und Molekularbiologie, Nussallee 11, D-53115 Bonn, Germany; <sup>3</sup>Zymenex A/S, Roskildevej 12 C, DK-3400 Hillerød, Denmark and Dalernum 13, S-18170 Lidingö, Sweden; <sup>4</sup>Research Center Borstel, Leibniz Center for Medicine and Biosciences, Parkallee 22, D-23845 Borstel; and <sup>5</sup>Children's Hospital, University of Hamburg, Martinistr. 52, D-20246 Hamburg, Germany

**Metachromatic leukodystrophy (MLD) is a lysosomal storage disease caused by a deficiency of the lysosomal enzyme arylsulfatase A (ASA). Enzyme replacement therapy (ERT) is a therapeutic option for MLD and other lysosomal disorders. This therapy depends on *N*-linked oligosaccharide-mediated delivery of intravenously injected recombinant enzyme to the lysosomes of patient cells. Because of the importance of *N*-linked oligosaccharide side chains in ERT, we examined the composition of the three *N*-linked glycans of four different recombinant ASAs in a site-specific manner. Depending on the culture conditions and the cell line expressing the enzyme, we detected a high variability of the high-mannose-type *N*-glycans which prevail at all glycosylation sites. Our data show that the composition of the glycans is largely determined by substantial trimming in the medium. The susceptibility for trimming is different for the glycans at the three *N*-glycosylation sites. Interestingly, which of the glycans is most susceptible to trimming also depends on production conditions. CHO cells cultured under bioreactor conditions yielded recombinant ASA with the most preserved *N*-glycan structures, the highest mannose-6-phosphate content and the highest similarity to non-recombinant enzyme. Notably, roughly one-third of the *N*-glycans released from the three glycosylation sites were fucosylated. In the last years, numerous recombinant lysosomal enzymes were used for preclinical ERT trials. Our data show that the oligosaccharide structures were very different in these trials making it difficult to draw common conclusions from the various investigations.**

**Keywords:** arylsulfatase A/enzyme replacement therapy/  
mannose 6-phosphate/metachromatic leukodystrophy

## Introduction

Arylsulfatase A (ASA, E.C. 3.1.6.8.) catalyzes the first step in the intralysosomal degradation of the sphingolipid 3-*O*-

sulfogalactosylceramide, briefly called sulfatide (von Figura et al. 2001). ASA is synthesized at the rough endoplasmic reticulum as a 62 kDa polypeptide and receives three *N*-linked oligosaccharide side chains at asparagine residues 158, 184, and 350 (Gieselmann et al. 1992). In the Golgi apparatus, the oligosaccharide side chains are modified by a phosphotransferase which specifically recognizes lysosomal glycoproteins and initiates the phosphorylation of mannose residues (Storch and Braulke, 2005). In a two-step process, this finally results in the generation of mannose 6-phosphate (M6P) residues. In recombinant ASA produced by BHK cells most likely only the *N*-glycans at positions 158 and 350 bear M6P residues (Gieselmann et al. 1992).

Deficiency of ASA causes intralysosomal accumulation of sulfatide and results in a lysosomal storage disorder (LSD) called metachromatic leukodystrophy (MLD). In MLD, sulfatide is stored in, e.g., kidney cells, oligodendrocytes, and Schwann cells (von Figura et al. 2001). Storage in the latter two results in demyelination which causes various finally lethal symptoms in the patients. For MLD and other LSDs, enzyme replacement therapies (ERTs) are under clinical investigation. For some diseases, they have already been clinically established and the respective enzyme has been approved for clinical use (Beck 2007). ERT is based on repeated intravenous injection of the active counterpart of the deficient enzyme. The rationale for this approach is that lysosomal enzymes can bind to M6P receptors at the plasma membrane resulting in efficient endocytosis of receptor/enzyme complexes, delivery of active enzyme to the lysosomal compartment, and correction of the metabolic defect (Storch and Braulke 2005). The relevance of the M6P receptor-mediated pathway for correction has been demonstrated by cell culture experiments in which reduction of storage material from patient cells was abolished by the addition of M6P to the culture medium or by pretreatment of enzyme with alkaline phosphatase (Sly 2002).

Therefore, it has been assumed that the most important pharmacological feature for therapeutic efficacy of a lysosomal enzyme is its content of M6P. However, preclinical ERT studies using mouse models of different LSDs did not consistently support this notion. Whereas studies on  $\beta$ -glucuronidase have demonstrated correlation of therapeutic efficacy with the M6P content (Sands et al. 2001), in  $\alpha$ -mannosidosis the least phosphorylated enzyme was the most effective (Roces et al. 2004). Oligosaccharide structures other than M6P residues, therefore, may have a strong impact on the therapeutic outcome of ERT and may outweigh inefficient M6P-dependent cellular uptake.

It is known from therapeutic glycoproteins of non-lysosomal origin that the glycosylation pattern can play important structural and functional roles by determining, e.g., conformation, oligomerization, stability, solubility, activity, immunogenicity, and plasma half life of glycoproteins (Donahue et al. 1986;

<sup>1</sup>To whom correspondence should be addressed: Tel: +49-228-735046; Fax: +49-228-732416; e-mail: matzner@ibmb.uni-bonn.de

Fukuda et al. 1986; Feizi and Childs 1987, Weiss and Ashwell 1989, Pohl et al. 2009). The pharmacokinetic and pharmacodynamic properties of lysosomal enzymes are determined by their *N*-glycans in a similar way (Pohl et al. 2009). Since LSDs are multisystemic disorders affecting different cell types, the biodistribution of injected lysosomal enzymes has been in the focus of some investigations. In type I Gaucher disease substrate accumulates in reticuloendothelial cells (for a review see Jmoudiak and Futerman (2005)). Early ERT studies used a therapeutic enzyme ( $\beta$ -glucosidase) with a high content of complex-type *N*-glycans. These structures mediated preferential uptake of enzyme by non-storing hepatocytes resulting in the absence of therapeutic benefit. The problem was subsequently solved by pretreating  $\beta$ -glucosidase with exoglycosidases to expose the core-mannose residues. The mannose-terminated enzyme, which has been clinically approved, binds mainly to mannose receptors of reticuloendothelial cells and substantially increases therapeutic efficacy.

Carbohydrate remodeling has also been used to increase the poor accessibility of the central nervous system for the therapeutic enzyme (Grubb et al. 2008). In this preclinical study, the terminal sugars of  $\beta$ -glucuronidase were modified by periodate treatment followed by borohydride reduction. The modified enzyme proved to be more efficient in penetrating the blood–brain barrier and clearing storage material from neocortical neurons of mice than native  $\beta$ -glucuronidase. Preliminary data using a cell culture model of the blood–brain barrier indicate that also the transendothelial transfer rate of recombinant human ASA is carbohydrate dependent. Thus, deglycosylation of ASA by treatment with endoglycosidase H reduced transfer rates by approximately 50% (unpublished data). These are important findings because most LSDs affect the central nervous system, and delivery of the therapeutic enzyme across the blood–brain barrier is a major challenge in this field.

A wide variety of factors during the production of a recombinant protein can influence the composition and quantity of oligosaccharide side chains (Andersen and Goochee 1994; Gawlitzek et al. 1995). These factors include the cell line used for production, the growth status of producer cells, additions to the medium, cell culture methodology, and others. Due to our interest in optimizing ERT of MLD (Matzner et al. 2005, 2009) and the relevance of carbohydrates for therapeutic efficacy, we analyzed the composition of *N*-glycans of recombinantly expressed human ASA. In addition, ASAs produced under different conditions and in different cell lines were studied. We analyzed the composition, structure, and quantity of the oligosaccharide side chains separately at the three different *N*-glycosylation sites. In the future, we plan to use the various enzymes for direct comparative *in vivo* studies in a mouse model of MLD. This may allow us to correlate glycosylation patterns with therapeutic efficacy and to optimize production conditions for the therapeutic enzyme.

## Results

Four different ASA preparations were analyzed in this study. Table I summarizes producer cell lines, production conditions, and enzyme sources.

**Table I.** ASA preparations used in this study.

Designation	Producer cell line	Culture conditions	ASA source
BHK-ASA	BHK (Hamster)	Flask culture, serum <sup>a</sup>	Medium
HT1080-ASA	HT1080 (Human)	Flask culture, serum <sup>a</sup>	Medium
CHO-ASA	CHO (Hamster)	Flask culture, serum <sup>a</sup>	Medium
CHO-ASA-BR	CHO (Hamster)	Bioreactor, serum-free	Medium

<sup>a</sup>Fetal calf serum (1.5%).

### *Separation of oligosaccharide side chains*

ASA contains three potential *N*-glycosylation sites at amino acid residues Asn158 (G1), Asn184 (G2), and Asn 350 (G3), all of which are glycosylated (Gieselmann et al. 1992). To analyze the site-specific *N*-glycan structures, ASA to be analyzed was reduced, alkylated, desalted, and digested with trypsin. Tryptic peptides were separated by RP-HPLC. Figure 1A shows a typical elution profile of tryptic peptides which proved to be very reproducible for different ASA preparations and various column runs. In order to identify the fractions containing the glycosylated peptides, an aliquot of each HPLC-fraction was digested with PNGase F. The mass/charge profiles of undigested and digested aliquots were determined by MALDI-TOF mass spectrometry and compared with the calculated mass/charge ratios of fragments predicted from a theoretical trypsin digest of ASA. Predictable fragments which were present in PNGase F-treated aliquots, but absent in untreated samples were indicative of glycopeptides. As an example, the two mass spectra of the fraction containing the tryptic peptide covering amino acid residues 303–367 and G3 are shown in Figure 1C and D. PNGase F digestion reveals a peptide with a mass/charge ratio of 6576.42 (Figure 1D) which corresponds to the predicted value of the unglycosylated peptide 303–367. No equivalent peptide is detectable in the untreated aliquot due to the increment of its mass/charge ratio by the covalently linked oligosaccharide (Figure 1C). The HPLC-peak representing peptide 303–367 is labeled with G3 in Figure 1A. Since there are no trypsin cleavage sites between glycosylation sites G1 and G2, we expected a single peptide encompassing the two most *N*-terminal *N*-glycosylation sites. This peptide was identified by PNGase F digestion and MALDI-TOF mass spectrometry in the HPLC-fraction labeled G1/2 (Figure 1A). To separate G1 and G2, the diglycosylated tryptic peptide was digested with the endopeptidase AspN and the reaction products were separated by a second RP-HPLC run (Figure 1B) (Schmidt et al. 1995). The two glycopeptides harboring G1 and G2, respectively, were identified as described before and are indicated in Figure 1B.

### *Site-specific structures of oligosaccharides of BHK-ASA*

First, we analyzed the oligosaccharide side chains of ASA produced in BHK cells (BHK-ASA). After purification of the three glycopeptides harboring G1, G2, and G3, the *N*-linked oligosaccharides were cleaved off by PNGase F digestion, fluorescently labeled and analyzed by normal-phase HPLC. Figure 2, top panel, shows the analytic run of oligosaccharides isolated from G1 of BHK-ASA as an example. The most prominent peaks eluted at 6.25, 7.23, and 8.09 glucose units (GU). According to literature data (Guile et al. 1996; Arnold et al. 2004) and oligosaccharide standards which were analyzed by us in parallel (not shown), these GU-values indicate Hex<sub>5</sub>GlcNAc<sub>2</sub>, Hex<sub>6</sub>GlcNAc<sub>2</sub>, and Hex<sub>7</sub>GlcNAc<sub>2</sub>

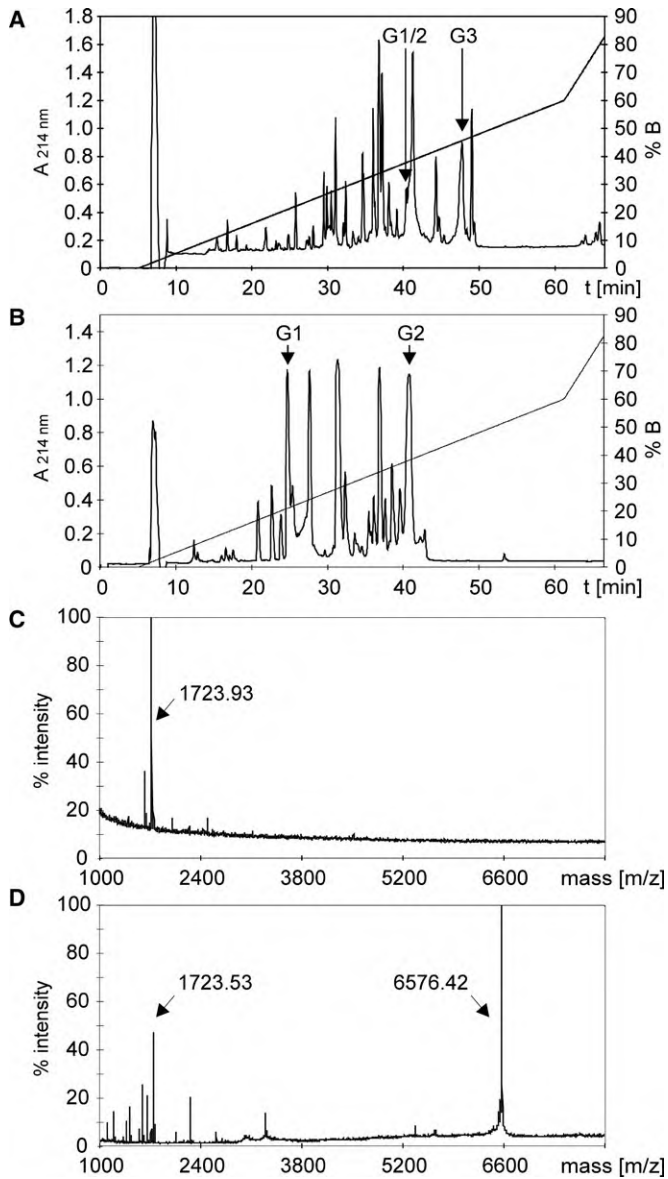


**Fig. 1.** RP-HPLC separation of tryptic peptides released from CHO-ASA-BR. (A) Elution profile of tryptic ASA fragments separated on a reversed phase C12 column. Glycopeptides were identified by PNGase F treatment as described below. The peak representing the tryptic peptide covering amino acid residues 144–200 and the first two *N*-glycosylation sites is indicated by G1/2. The peptide covering amino acid residues 303–367 and the third *N*-glycosylation site is labeled with G3. (B) Separation of *N*-glycosylation sites G1 and G2. Fractions containing the tryptic peptide with G1/2 were pooled and digested with AspN to separate the two *N*-glycosylation sites. The AspN digest was rechromatographed on a reversed C12 column. Fractions containing the glycopeptides covering the first (G1) and the second glycosylation sites (G2) are indicated. (C, D) Identification of glycopeptides by PNGase F treatment. Aliquots of all fractions obtained by HPLC were treated with PNGase F to cleave *N*-linked oligosaccharides from glycopeptides. Subsequently, the PNGase-treated and -untreated aliquots were compared by MALDI-TOF mass spectrometry. As an example, the spectra of the fraction containing the peptide covering G3 is shown prior (C) and after PNGase digestion (D). A peak with a mass/charge ratio of 6576.42 is visible only after PNGase treatment and equals the mass/charge ratio of the unglycosylated peptide harboring *N*-glycosylation site 3 as predicted from a theoretical trypsin digest of ASA. By contrast, a peak at 1723.93 is detectable in the digested and undigested sample and therefore indicates an unglycosylated tryptic ASA peptide (amino acid residues 98–114, calculated mass/charge ratio of 1723.96). Fractions containing the two peptides covering G1 and G2 were identified accordingly (not shown).

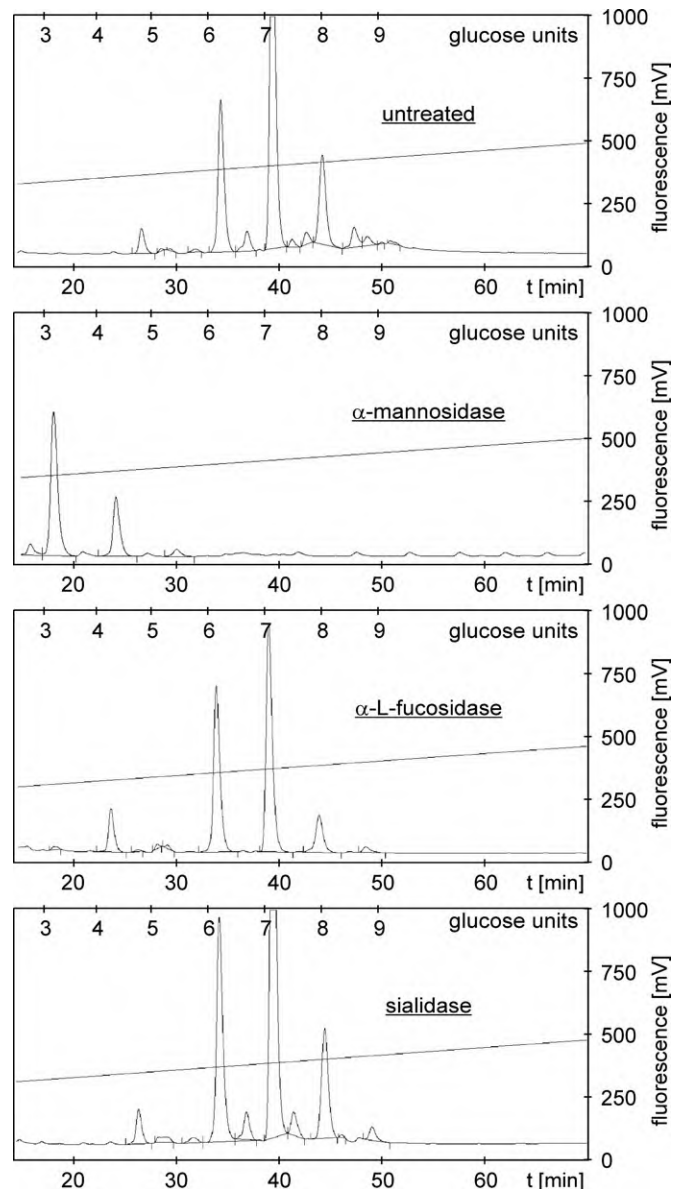


**Fig. 2.** Analysis of fluorescently labeled oligosaccharides of G1 of BHK-ASA. Oligosaccharides purified from G1 of BHK-ASA were fluorescently labeled and analyzed on an amide-80 column. The column was eluted with a gradient of 30–50% ammonium formate, pH 4.4, in acetonitrile. The elution time on the x-axis is plotted against the fluorescence on the y-axis. Arbitrary fluorescence units are in mV. The elution times of glucose polymers used as standards are indicated as glucose units on top. To specify their composition, oligosaccharides were subsequently digested with  $\alpha$ -mannosidase,  $\alpha$ -L-fucosidase, or sialidase as indicated. A comparison of the elution profiles of digested and undigested oligosaccharides indicates a prevalence of high-mannose-type *N*-glycans with a comparably high proportion of fucose residues.

structures. For a more precise analysis of the *N*-glycans, each labeled oligosaccharide preparation was split into six aliquots which were digested with  $\alpha$ -mannosidase,  $\alpha$ -fucosidase,  $\beta$ -galactosidase,  $\beta$ -hexosaminidase, sialidase, and phosphatase, respectively. The reaction products were analyzed by normal-phase HPLC. After  $\alpha$ -mannosidase digestion, signals eluting between 5 and 9 GU had vanished almost completely

(Figure 2, second panel). This indicates that mannose residues predominate at G1 and that the oligosaccharides are mainly of the high-mannose-type  $\text{Man}_5\text{GlcNAc}_2$ ,  $\text{Man}_6\text{GlcNAc}_2$  and  $\text{Man}_7\text{GlcNAc}_2$ . Digestion with  $\alpha$ -fucosidase led to the loss of various smaller peaks occurring in between the peaks representing the  $\text{Man}_{5-7}\text{GlcNAc}_2$  structures (Figure 2, third panel). This means that a considerable fraction of the high-mannose-type oligosaccharide at G1 of BHK-ASA is fucosylated. A few small peaks disappeared after sialidase treatment indicating that only a small fraction of oligosaccharides is of the complex type (Figure 2, bottom panel). Treatment with  $\beta$ -galactosidase,  $\beta$ -hexosaminidase, and phosphatase did not result in significant alterations of the elution profile (not shown). To estimate the fraction of fucosylated and sialylated *N*-glycans, the peak areas which were lost from the initial elution profile after  $\alpha$ -fucosidase or sialidase treatment were integrated. This quantitative evaluation indicated that  $\sim 6\%$  and  $\sim 2\%$  of the *N*-glycans were fucosylated and sialylated, respectively. *N*-Glycans at G2 and G3 were analyzed by the same procedure. The HPLC elution profiles of the undigested oligosaccharides present at the three individual *N*-glycosylation sites are compared on the left side of Figure 3. Treatment with the six enzymes used in the case of G1 was also performed with oligosaccharides cleaved from G2 and G3 (data not shown). In addition, unlabeled oligosaccharides of G1, G2, and G3 were separately analyzed by MALDI-TOF mass spectrometry. Spectra are shown in the right part of Figure 3. The oligosaccharide structures revealed by mass spectrometry are in good agreement with those detected by HPLC analysis of labeled oligosaccharides. Thus, MALDI-TOF analysis confirms a very low concentration of complex- or hybrid-type oligosaccharides by showing only weak signals characteristic of such structures (boxed structures in Figure 3, right panel). Data of the HPLC and mass spectrometry analysis of BHK-ASA are shown in supplementary Table I. At G1 more than 70% of the oligosaccharide side chains have six or more mannoses, the most frequent displaying a  $\text{Man}_6\text{GlcNAc}_2$  structure. Only 3% are oligosaccharides with less than four mannoses. At G2, only 35% have at least six mannoses, but considerable 34% less than four. Similarly at G3, 31% are at least  $\text{Man}_6\text{GlcNAc}_2$  structures but 22% have less than four mannoses. Thus, the high-mannose-type oligosaccharide side chains are well preserved at G1 whereas oligosaccharides at G2 and G3 are shorter on average. A considerable fraction of oligosaccharides is fucosylated, 11% at G1 and 14–15% at G2 and G3, respectively.

#### *Global analysis of oligosaccharides of BHK-ASA*

The data about the frequencies of the different oligosaccharide structures at G1, G2, and G3, allowed us to calculate that one BHK-ASA molecule carries 21.6 monosaccharides on average. As a control for the methodology used for the site-specific analysis of oligosaccharide side chains, monosaccharides were collectively released from the *N*-glycans of BHK-ASA by acid hydrolysis, fluorescently labeled and quantified by RP-HPLC (not shown). This global analysis yielded a mean of 20.3 monosaccharides per ASA molecule and thus confirmed the accuracy of the site-specific analysis. The global analysis was also used to reanalyze the seemingly low M6P content of BHK-ASA. In contrast to the site-specific analysis which failed to demonstrate M6P, the global analysis detected 0.9 M6P residues per ASA molecule on average. This discrepancy might be explained by

a hydrolytic loss of M6P during the processing of samples for the site-specific analysis. This notion is supported by our observation that the M6P content of ASA declines under conditions of low ionic strength. Thus, ASA had  $>90\%$  less M6P when it was transferred from the storage buffer to water and stored for 2 months compared to the same enzyme preparation when it was transferred from the storage buffer to water at the day before RP-HPLC analysis (not shown). Although, the loss of M6P was not systematically analyzed, the data suggested that our protocol for the site-specific analysis of *N*-glycans substantially underestimates the M6P concentration. To circumvent this limitation, the M6P content of ASA was measured by independent assays (see below).

#### *Site-specific structures of oligosaccharides of CHO-ASA-BR*

Next we analyzed the preparation of ASA produced in CHO cells which was used in the preclinical enzyme replacement trials published (Matzner et al. 2005, 2009). This ASA was prepared from CHO cells grown under industrial bioreactor conditions and is here designated as CHO-ASA-BR. HPLC elution profiles of the oligosaccharides cleaved from the three *N*-glycosylation sites are shown in Figure 4, left panel, and are quantitatively summarized in supplementary Table II. Data were obtained by exoglycosidase treatment as described for BHK-ASA (not shown). The analyses revealed that CHO-ASA-BR has well preserved high-mannose-type oligosaccharide side chains. At G1 and G3, 87% and 96% of the *N*-glycans have six or more mannoses, respectively. At these sites, oligosaccharides with less than five mannoses could not be detected at all. At G2, oligosaccharide appeared to bear slightly less mannose residues. Thus, 33% had at least six mannoses and 3.7% had less than four. In addition, CHO-ASA-BR shows a high degree of fucosylation ranging from 22% at G3 to 33% at G2 and 41% at G1.

#### *Site-specific structures of oligosaccharides of HT1080-ASA and CHO-ASA*

To examine the factors which determine the site-specific structures of the oligosaccharide side chain, we also analyzed the *N*-glycan composition of ASA expressed in HT1080 cells (HT1080-ASA) and in CHO cells which were grown in flasks under conventional cell culture conditions (CHO-ASA). Figure 4 shows the HPLC elution profiles of fluorescently labeled oligosaccharides isolated from G1, G2, and G3 of HT1080-ASA (middle panel) and CHO-ASA (right panel), respectively. As described for BHK-ASA and CHO-ASA-BR, the HPLC-analysis was repeated after exoglycosidase digestion (data not shown). Data for HT1080-ASA are summarized in supplementary Table III. In general, the oligosaccharide side chains of HT1080-ASA contain fewer mannoses than those of BHK-ASA. Thus, only 8.3% and 2.7% of the *N*-glycans at G1 and G2 of HT1080-ASA have six or more mannoses, respectively. At G3, the percentage is higher (22.9%) but still does not reach the values of BHK-ASA. As for BHK-ASA, a substantial fraction of oligosaccharides is fucosylated. A striking difference in the fucose concentration is, however, detectable at G3 where HT1080-ASA bears 4-fold more fucose residues than BHK-ASA. In contrast, the *N*-glycans of CHO-ASA which was produced under the same conditions as BHK- and HT1080-ASA were heavily trimmed (Figure 4, right panel, and supplementary Table IV). Less than

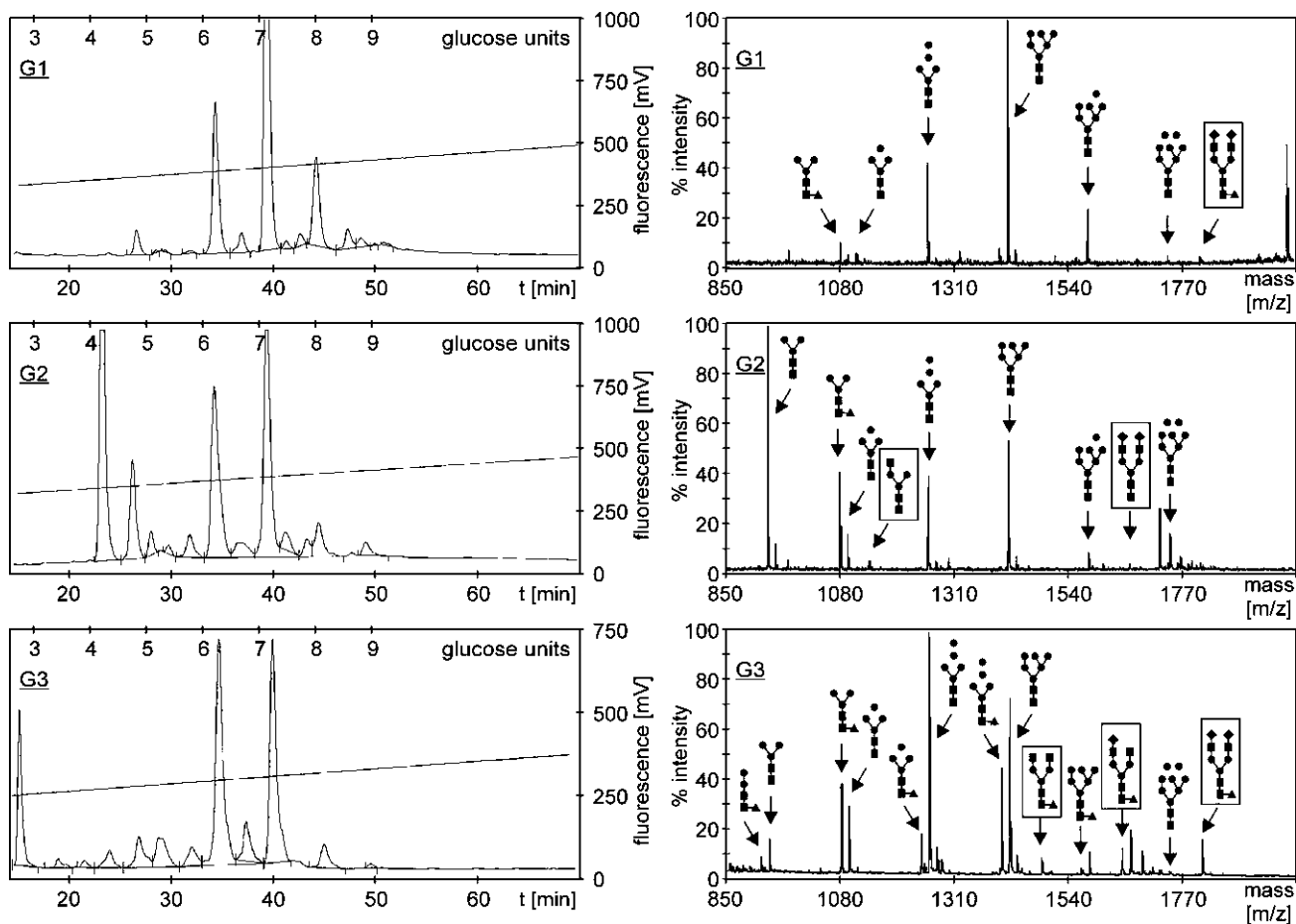


**Fig. 3.** Composition of oligosaccharide side chains of BHK-ASA. G1, G2, and G3 were isolated from ASA produced in BHK cells. Oligosaccharides were analyzed by MALDI-TOF mass spectrometry (right part) and in parallel on a amide-80 HPLC after fluorescent labeling (left part). In the right part, some characteristic oligosaccharide structures determined by mass spectrometry are schematically indicated. Complex- and hybrid-type structures are boxed. Squares: *N*-acetylglucosamin, circles: mannose, triangles: fucose, diamonds: galactose. For a summary of results see supplementary Table I.

2% of the side chains had six or more mannoses whereas at G1 87%, at G2 77%, and at G3 59%, respectively, of the side chains had less than four mannoses. Fucosylation at G1 was undetectable. However, 8.0% and 13.2% of the oligosaccharides were fucosylated at G2 and G3, respectively.

#### *Trimming of oligosaccharides by a conditioned medium*

The structure of *N*-glycans of ASAs produced under conventional cell culture conditions suggested that high-mannose-type *N*-glycans are trimmed extracellularly by glycosidases present in the media. Therefore, we determined glycosidase activities in the medium of the three cell lines which had been used for enzyme production (Figure 5). These data show that CHO cells produce the highest amount of  $\alpha$ -mannosidase activity, whereas BHK cells produce the least. HT1080 cells have intermediate activity. This is in agreement with our finding that the number of mannose residues declines from BHK-ASA to HT1080-ASA and to CHO-ASA. To proof that *N*-glycans are extensively modified after ASA has been secreted into the medium, we incubated purified BHK-ASA for 4 days at 37°C with either non-conditioned medium or medium conditioned by CHO cells. After incubation and re-purification, we performed a global analysis of the oligosaccharide structures. When BHK-ASA had been

incubated in a fresh medium, 46% of the pooled oligosaccharides had six or more mannoses and structures with less than three mannoses were undetectable (Figure 6, upper panel). After incubation with the conditioned medium, however, none of the oligosaccharide side chains had more than five mannoses and 63% had no mannose left at all (Figure 6, lower panel). In addition, there were no fucose residues detectable after incubation in the conditioned medium (not shown).

#### *Analysis of M6P concentrations*

Since the method used for the site-specific analysis of *N*-glycans did not allow for a precise quantification of M6P (see above), the global M6P content of ASA was determined by alternative assays. In a first experiment, M6P was quantified by RP-HPLC of derivatized monosaccharides collectively released from the three *N*-glycans of ASA. Derivatized M6P of known concentrations were used as standards. This assay revealed 0.9 mol M6P per mol BHK-ASA and 2.6 mol/mol for CHO-ASA-BR (not shown). In a second experiment, inorganic phosphate released from the M6P groups by ashing was measured by a highly sensitive malachite green phosphate assay (Buss and Stull 1983). As a control we used  $\alpha$ -galactosidase A (Replagal™ from Shire, Hamshire, UK) which has been reported to have a M6P

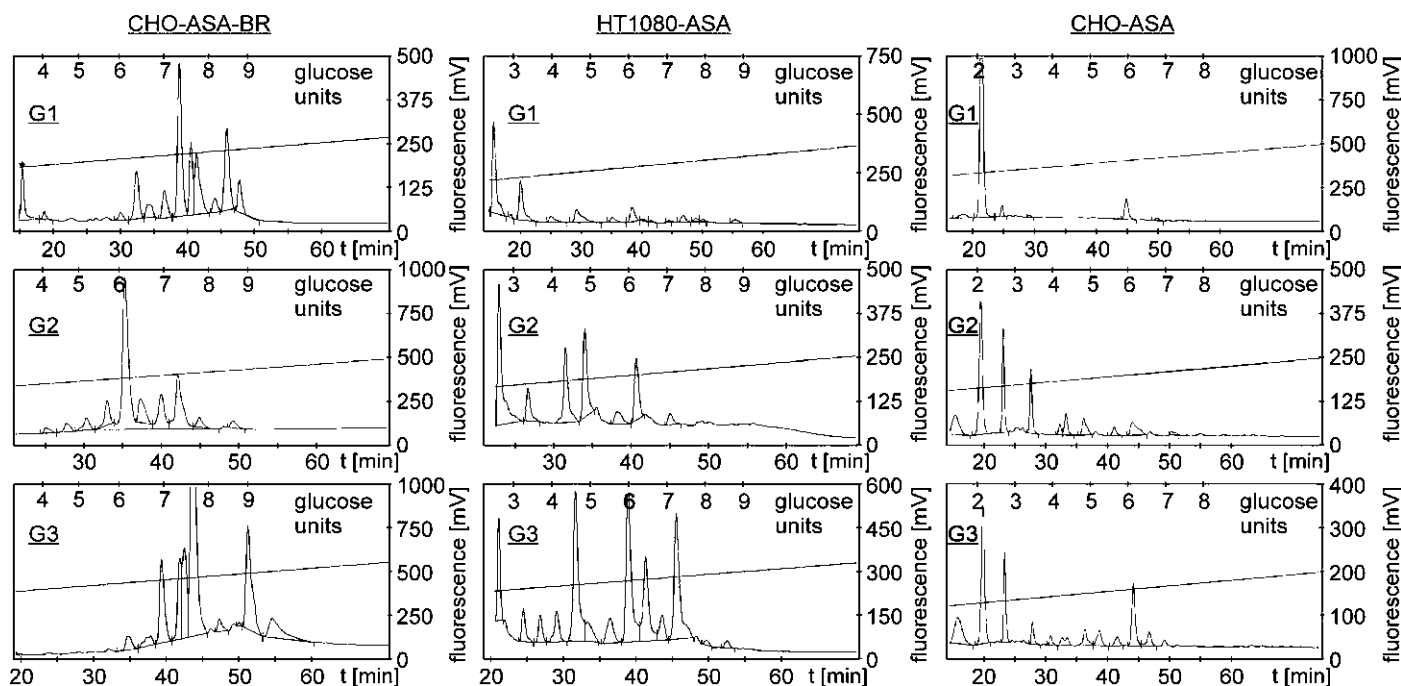


**Fig. 4.** Composition of oligosaccharide side chains of CHO-ASA-BR, HT1080-ASA, and CHO-ASA. Oligosaccharide side chains of glycosylation sites G1, G2, and G3 were isolated from ASA produced by CHO cells cultured under bioreactor conditions (left panel), HT1080 cells cultured under conventional cell culture conditions (middle panel) or by CHO cells cultured under conventional cell culture conditions (right panel). Oligosaccharides were analyzed on an amide-80 HPLC column after fluorescent labeling. HPLC analysis of aliquots treated with  $\alpha$ -mannosidase,  $\alpha$ -fucosidase,  $\beta$ -galactosidase,  $\beta$ -hexosaminidase, sialidase or phosphatase allowed the identification and quantification of the different oligosaccharide structures present at G1, G2, and G3 (not shown). For a summary of the results, see supplementary Tables II–IV.

content of 1.3 mol/mol (Sakuraba et al. 2006). In three independent assays, we detected  $1.4 \pm 0.13$ ,  $1.0 \pm 0.07$ ,  $1.3 \pm 0.02$ , and  $3.4 \pm 0.08$  mol/mol M6P for  $\alpha$ -galactosidase A, HT1080-ASA, BHK-ASA, and CHO-ASA-BR, respectively (mean  $\pm$  SD). This result could be partially confirmed by a third assay utilizing a novel single chain  $\alpha$ -M6P antibody for immunoblotting. For this analysis, equal amounts of different ASA preparations were separated by SDS–PAGE and transferred to a nitrocellulose transfer membrane. M6P was detected by sequential incubation of the membrane with a myc-tagged  $\alpha$ -M6P antibody, peroxidase-conjugated  $\alpha$ -myc mouse IgG (Sigma-Aldrich, Munich, Germany, M5546), and ECL Western blotting substrate (Thermo Fisher Scientific, Bonn, Germany). Densitometric analysis of signal intensities revealed M6P ratios of 1.0:1.3:3.2 between HT1080-ASA, BHK-ASA, and CHO-ASA-BR (not shown). It has to be mentioned that signals for  $\alpha$ -galactosidase were substantially lower than expected from the previous experiment. This may be explained by enzyme-specific differences in the steric arrangement of M6P groups. Thus, it is conceivable that two closely adjacent M6P residues are unable to bind two  $\alpha$ -M6P antibodies simultaneously leading to an underestimation of the M6P content.

## Discussion

We performed a detailed site-specific analysis of the three oligosaccharide side chains of ASA produced recombinantly in three cell lines and under two different culture conditions. Our data revealed the structures and relative quantities of the

various oligosaccharides at the different *N*-glycosylation sites. The initial focus of our studies was on bioreactor-produced ASA (CHO-ASA-BR) which was used in previous ERT trials in a mouse model of MLD (Matzner et al. 2005, 2009). An enzyme which is produced under similar conditions is currently evaluated for therapeutic efficacy in a clinical phase I/II study in patients with MLD.

Our study indicates that more than 97% of all *N*-glycans released from CHO-ASA-BR are of the high mannose type. The prevalence of high-mannose structures is in accordance with previous data obtained for non-recombinant ASA (Laidler and Litynska 1997; Hoja-Lukowicz et al. 2000). Thus, no hybrid- and complex-type oligosaccharides could be detected by MALDI mass spectrometry in the global glycan pool released from placental ASA. High-mannose structures also prevail in other lysosomal enzymes and this type of *N*-glycans has been implicated in promoting stability against intralysosomal proteolysis (Faid et al. 2006). The abundance of high-mannose-type oligosaccharides in ASA and other lysosomal enzymes may be due to phosphorylation of mannose residues, a modification which is initiated in a pre-Golgi compartment and prevents processing of *N*-glycans to complex-type oligosaccharides in the Golgi apparatus (Pohl et al. 2009). The majority of oligosaccharides present at the three glycosylation sites of CHO-ASA-BR have at least six mannoses (Figures 7, 8). The most dominant peak obtained by MALDI mass spectrometry of placental ASA-derived oligosaccharides represented a (fucosylated)  $\text{Man}_3\text{GlcNAc}_2$  structure (Hoja-Lukowicz et al. 2000). Prominent peaks were, however, also detectable for high-mannose oligosaccharides with six or more mannoses residues. Such large

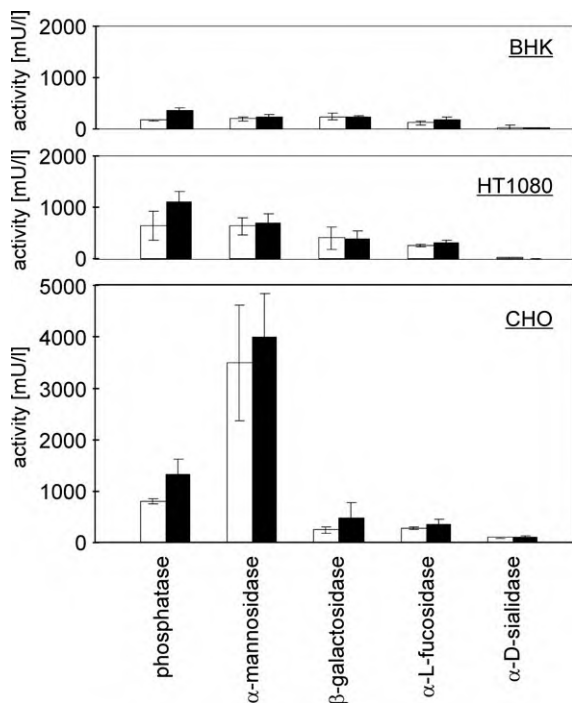


**Fig. 5.** Activities of various glycosidases in secretions of different cell types. The activities of  $\alpha$ -mannosidase, phosphatase,  $\beta$ -galactosidase,  $\alpha$ -L-fucosidase, and  $\alpha$ -D-sialidase were measured in a medium which had been conditioned for 4 (open bars) or 8 days (closed bars) by BHK, HT1080, and CHO cells, respectively, cultured under conventional flask conditions. The activities were measured at the pH value of the conditioned medium which ranged cell type specifically between pH 6.0 and pH 7.0. Bars represent means  $\pm$  SDs of three measurements.

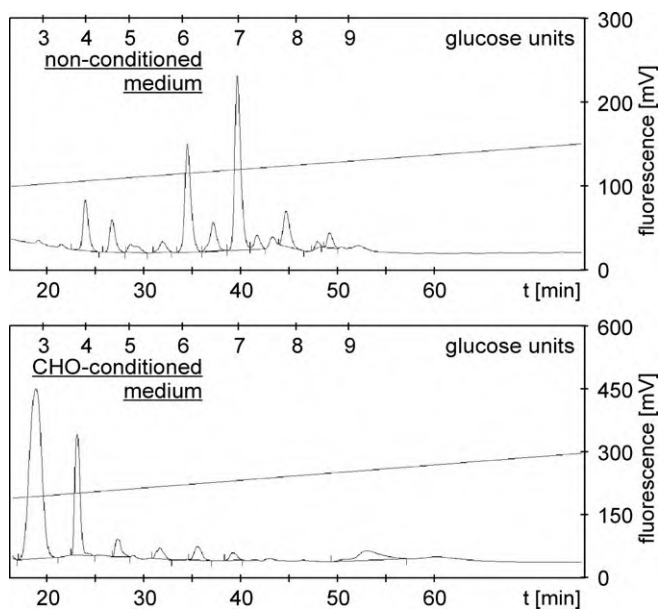


**Fig. 6.** Degradation of oligosaccharides in the conditioned medium. BHK-ASA (100  $\mu$ g) was incubated for 4 days at 37°C in 2 mL of either fresh medium (upper panel) or medium which had been conditioned by CHO cells for 8 days (lower panel). After repurification of the incubated ASA, the oligosaccharide side chains were isolated (without separation of G1, G2, and G3), fluorescently labeled, and analyzed on an amide-80 HPLC column. Main peaks of the fluorescence profiles indicate Man<sub>5</sub> and Man<sub>7</sub> structures (upper panel) and Man<sub>1</sub> and Man<sub>2</sub> structures (lower panel).

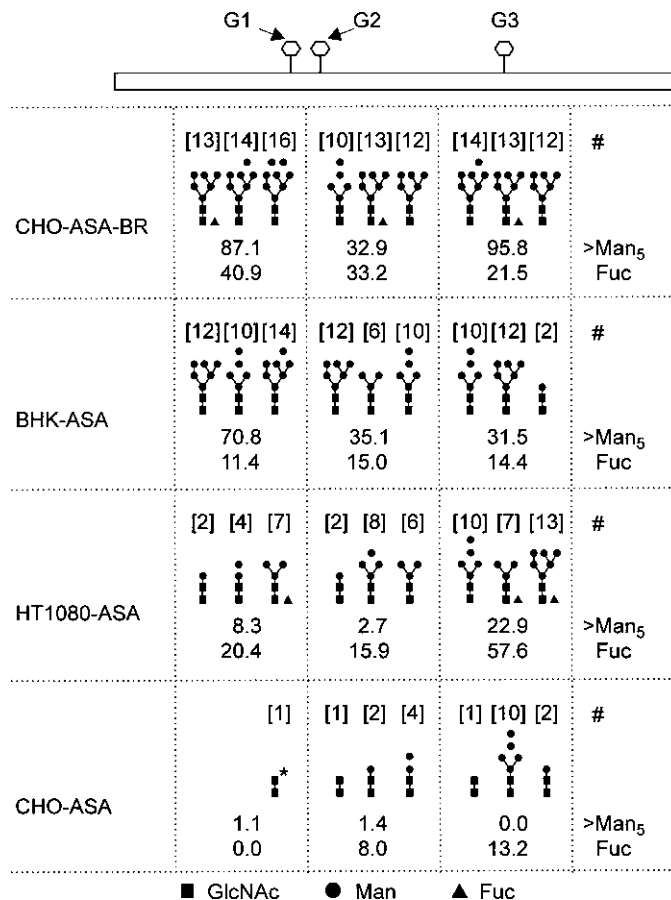


**Fig. 7.** Schematic presentation of oligosaccharide structures in the various ASAs. A schematic drawing of the ASA glycoprotein is shown in the top panel. The bar indicates the ASA polypeptide backbone. Hexagons represent the positions of the three oligosaccharide side chains at Asn158 (G1), Asn 184 (G2), and Asn350 (G3), respectively. For each of the four ASA preparations indicated on the left, the three oligosaccharide structures which prevail at G1, G2, and G3 are schematically shown. The fucose residue of fucosylated structures is drawn adjacent to the innermost GlcNAc. Please note that linkage of the fucose to this GlcNAc residue has not been experimentally proven. For each triplicate, the frequency of the oligosaccharides declines from left to right. For details about frequencies of the indicated as well as less abundant structures see supplementary Tables I–IV. Numbers in square brackets above the structures refer to sequential oligosaccharide numbers used in the tables. Numbers below the structures indicate the percentage of oligosaccharides with at least six mannoses and the degree of fucosylation, respectively. Asterisk – alternative structures make up less than 10% of the oligosaccharides at G1 of CHO-ASA-C and are therefore not shown.

oligosaccharides are likely to be attached to newly synthesized ASA molecules before they are trimmed during transport and processing in the tissue. Thus, the oligosaccharide structures of secreted CHO-ASA-BR is well preserved and the number of mannose residues added to the placental enzyme during its biosynthesis seems to be similar to that of CHO-ASA-BR.

Interestingly, a considerable fraction of the oligosaccharides released from CHO-ASA-BR was found to be fucosylated. The degree of fucosylation ranged between 22% at G3 and 41% at G1 (Figure 7). In mammalian *N*-glycans, fucose can be linked to galactose or *N*-acetylglucosamin residues of outer arms or to the innermost *N*-acetylglucosamin residue (Staudacher et al. 1999). For CHO-ASA-BR, *N*-glycans with terminal or

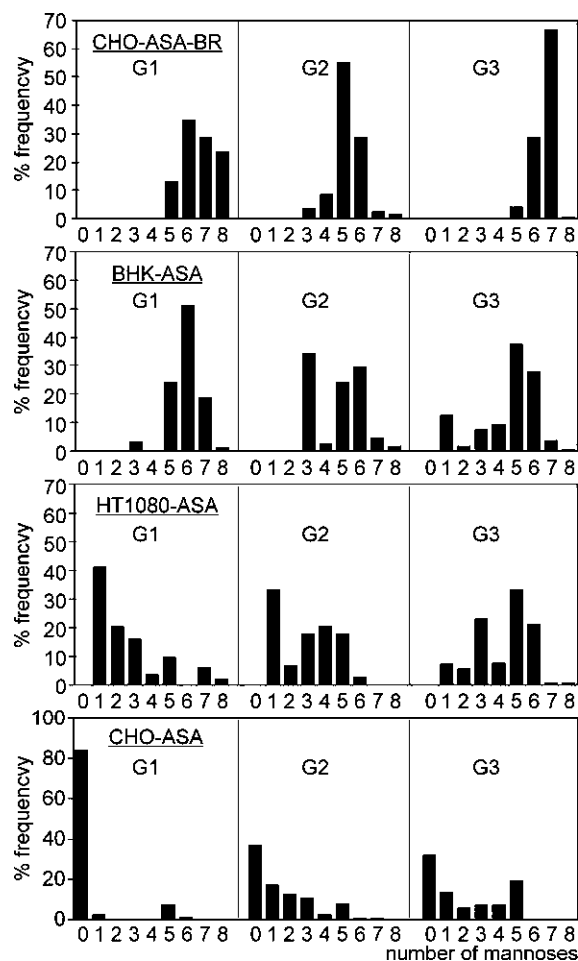


**Fig. 8.** Heterogeneity of *N*-linked oligosaccharide side chains. For each of the oligosaccharide side chains at G1, G2, and G3 of the different ASAs, the number of mannoses on the x-axis is plotted against the frequency (%) of corresponding structures on the y-axis. Please note that some minor peaks obtained in the HPLC analysis could not be attributed to distinct oligosaccharide structures. Depending on the glycosylation site, the frequency of such non-identifiable structures ranged between 0.01% and 4.3% (for details see supplementary Tables I–IV). This explains why the sum of the indicated frequencies is smaller than 100%.

subterminal galactose or *N*-acetylglucosamin residues are scarce and account for less than 3% of all oligosaccharides. Due to the low concentration of structures which may serve as substrates for outer-arm fucosylation and the high concentration of fucose attached to the *N*-glycans, ASA is most likely core-fucosylated. Although not yet experimentally proven, this notion is supported by the presence of smaller fucosylated oligosaccharides which bear only the two inner *N*-acetylglucosamine residues and three or less mannose residues (see supplementary Tables II and III). Further evidence for core fucosylation of ASA comes from exoglycosidase sequencing and lectin affinity chromatography of placental ASA-derived *N*-glycans which suggested that almost half of the high-mannose-type oligosaccharides contained 6-*O*-*L*-fucose bound to the innermost *N*-acetylglucosamine residue (Laidler et al. 1994; Hoja-Lukowicz et al. 2000). Of note, core-fucosylated oligomannose-type structures have also been described for five other lysosomal enzymes (cathepsin B, cathepsin H, cathepsin D,  $\beta$ -glucuronidase,  $\alpha$ -mannosidase) suggest-

ing that this type of modification may be related to the proper operation of acid hydrolases (Howard et al. 1982; Takahashi et al. 1983; Taniguchi et al. 1985; Kozutsumi et al. 1986). Core fucosylation is catalyzed by the *N*-acetyl  $\beta$ -D-glucosaminide  $\alpha$ -(1,6)-fucosyltransferase. This enzyme has been reported to accept complex and hybrid oligosaccharides as a substrate, but not high-mannose-type oligosaccharides (Voynow et al. 1991). It is therefore surprising that the high-mannose-type oligosaccharides of ASA and possibly other lysosomal enzymes may serve as a substrate for core fucosylation. Furthermore, the  $\alpha$ -(1,6)-fucosyltransferase is believed to be localized to the medial Golgi apparatus. The largest fucosylated structure which we could detect in CHO-ASA-BR was [Fuc]Man<sub>8</sub>GlcNAc<sub>2</sub> accounting for roughly 6% of all *N*-glycans at G1 (see supplementary Table II). This suggests that against the current view Man<sub>8</sub>GlcNAc<sub>2</sub> glycans are a substrate of the  $\alpha$ -(1,6)-fucosyltransferase and that core fucosylation has therefore to occur in the endoplasmic reticulum or the *cis*-Golgi apparatus.

The comparison of recombinant BHK-ASA-BR and non-recombinant ASA isolated from human placenta suggests that CHO-ASA-BR closely resembles placental ASA with respect to fucosylation, mannosylation, and sialylation of its oligosaccharide side chains. A striking difference between the two ASAs is, however, the concentration of M6P residues. While M6P residues were undetectable in placental ASA (Hoja-Lukowicz et al. 2000), the *N*-glycans of CHO-ASA-BR bear 3.4 mol M6P per mol enzyme. M6P residues which are added to newly synthesized ASA and other soluble lysosomal enzymes are essential for the targeting of these glycoproteins to lysosomes where M6P residues are rapidly removed by the acid phosphatase 5 (Storch and Braulke 2005; Sun et al. 2008; Pohl et al. 2009). ASA has an intralysosomal half life of several weeks and, therefore, the majority of ASA purified from placenta is expected to be of lysosomal origin. Consequently, the lack of M6P may be explained by the dephosphorylation of initially phosphorylated ASA in the lysosomal compartment.

The analysis of recombinant ASAs other than CHO-ASA-BR revealed a surprisingly high variability of *N*-glycan structures. When ASA was purified from secretions of CHO cells which were maintained under conventional cell culture conditions (CHO-ASA) instead of being cultured in a bioreactor, *N*-glycans were heavily truncated. Actually, less than 2% of oligosaccharides released from G1, G2, or G3 of CHO-ASA contain at least six mannoses and 32–84% bears no mannose at all (Figures 7, 8). The culture condition of the producer cells therefore has a fundamental impact on the integrity of the oligosaccharides.

The *N*-glycan structures turned out to depend also on the cell line used for ASA production. Thus, when CHO-, HT1080-, and BHK-cells were cultured under the same conventional cell culture conditions, the BHK-ASA showed the most preserved oligosaccharide side chains (Figures 7, 8). Here 71%, 35%, and 32% of oligosaccharide side chains at position G1, G2, and G3 bear at least six mannoses, respectively. Oligosaccharide side chains of ASA secreted by HT1080 cells (HT1080-ASA) are intermediate: there are more mannose-rich oligosaccharides than in CHO-ASA, but less than in BHK-ASA. The truncated structure of the oligosaccharide side chains in particular of CHO-ASA can most likely be explained by extracellular trimming of the oligosaccharides by glycosidases present in the medium of these cells (Figure 5). Likewise, the decline of the M6P

concentration from CHO-ASA-BR to BHK-ASA and to HT1080-ASA might be ascribed to extracellular phosphatases which accumulate to different levels depending on producer cell type and culture conditions.

The impact of extracellular glycosidases on oligosaccharide structures is underscored by an experiment in which we incubated BHK-ASA with a medium conditioned by CHO cells. Although the ASA concentration was more than 50-fold higher in this experiment than in the medium of CHO cells cultured for ASA production, BHK-ASA oligosaccharide chains were substantially trimmed after 4 days of incubation (Figure 6). Similar observations have been made for non-lysosomal glycoproteins (Gramer and Goochee 1993; Gramer et al. 1995). Glycosidases delivered by CHO cells are active within a broad pH spectrum suggesting that they represent a mixture of lysosomal and cytosolic enzymes (Gramer and Goochee 1993). Our data suggest that the high integrity of the *N*-glycans of CHO-ASA-BR is most likely due to the continuous flow of the medium in the bioreactor which reduces both the accumulation of glycosidases and the average length of stay of recombinant ASA.

The site-specific analysis of the oligosaccharide side chains also revealed that there are positional effects which determine the degree of oligosaccharide trimming. The extent of trimming depends on producer cell type, *N*-glycan position, and sugar residue. In BHK-ASA, for example, G1 carries the most intact *N*-glycans as measured by the fraction of oligosaccharides with more than five mannoses (Figure 8). G3, in contrast, seems to be most susceptible to trimming. In HT1080-ASA, in contrast, G3 seems to be most resistant to trimming and G2 most sensitive. Thus, it is not consistently one particular oligosaccharide side chain which is most susceptible, but in different cell types the oligosaccharides at the various positions display different sensitivities for being trimmed. Cell type rather than species-specific differences in the expression of glycosidases and/or glycosyltransferases may account for this heterogeneity (Albach et al. 2001).

In the last years, ERT studies in a wide variety of animal models of different LSDs were performed. The lysosomal enzymes which were used in these studies were produced under different conditions, but mostly under standard laboratory conditions. In addition, a variety of cell lines were used such as CHO, HEK293, murine embryonic fibroblasts, and others. In some studies, the degree of phosphorylation was determined and it varies from as low as 4.6% for human  $\alpha$ -mannosidase (Roces et al. 2004) to as much as 95% for  $\beta$ -glucuronidase (Sands et al. 2001). Various studies have shown that enzymes from different sources differ in their therapeutic efficacy and pharmacokinetics. Thus, it was shown in a mouse model of  $\alpha$ -mannosidosis that the least phosphorylated human  $\alpha$ -mannosidase was therapeutically more efficient than the highly phosphorylated murine enzyme (Roces et al. 2004). Although  $\alpha$ -mannosidase from a bovine source bears similarly low phosphorylated oligosaccharide side chains than the human enzyme, it was still therapeutically less efficient. This suggests that in  $\alpha$ -mannosidosis therapeutic efficacy is primarily not determined by the degree of phosphorylation but by other so far unknown parameters. Similarly, it was shown in a cat model of MPS VI that feline arylsulfatase B was five times more efficient than human arylsulfatase B. The feline enzyme, however, was produced in a rapid flow bioreactor (Bieliński et al. 1999), whereas the human enzyme has been produced under standard laboratory conditions (Crawley et al.

1996). Thus, the differences in therapeutic efficacy in this study may not be due to species differences but rather due to differences in the production procedure. In these studies, little attention has so far been paid to the heterogeneity of the oligosaccharide side chains of the therapeutic enzymes. Our data suggest that in most of the animal studies in which the enzymes were produced under conventional cell culture conditions, oligosaccharide structures may have been heavily trimmed. We do not know, how trimmed oligosaccharide side chains influence therapeutic efficacy and pharmacokinetics of lysosomal enzymes. In fact, because oligosaccharide structures were neglected in the past, it may be difficult to compare results from different enzyme replacement studies and to draw common conclusions. Unrecognized differences in the structures of *N*-glycans linked to the various therapeutic enzymes may also explain the so far unsolved issue why ERT was effective in reducing brain storage in some studies, but not in others (e.g., Miranda et al. (2000); Roces et al. (2004); Matzner et al. (2005)).

## Materials and methods

### *Cell culture and protein purification*

Human arylsulfatase A (ASA) was stably expressed in three different cell lines: baby hamster kidney cells (BHK), Chinese hamster ovary (CHO) cells, and HT1080 human fibrosarcoma cells. BHK cells were cotransfected with the cDNAs of human ASA and human  $M_r$  46,000 M6P receptor and have been described before (Schmidt et al. 1995). CHO and HT1080 cells were transfected with the cDNAs of human ASA. Cotransfection with a neomycin resistance cassette allowed for the selection of stably transfected colonies. For flask culture, cells were cultivated in a DMEM medium (Invitrogen, Karlsruhe, Germany) supplemented with 1.5% fetal calf serum. The medium was harvested every 4 days and immediately precipitated with ammonium sulfate (50%, w/v). The precipitate was collected by centrifugation, dialyzed against 10 mM Tris/HCl pH 7.2/150 mM NaCl. This dialysate was passed over an immunoaffinity column to which a monoclonal  $\alpha$ -ASA antibody was coupled. Details of the procedure have been described elsewhere (Schierau et al. 1999). Production of ASA in the bioreactor was in perfusion mode in a serum-free ExCell 302 medium. ASA was purified by a combination of ion-exchange, hydrophobic interaction and affinity interaction chromatographic separation steps (for details see <http://www.freepatentsonline.com/y2008/0003211.html>).

### *Tryptic digestion of ASA*

One hundred micrograms of protein was dried in a Savant SpeedVac SC100 (Savant Instruments Inc., Farmingdale, NY) and resuspended in a 125  $\mu$ L RCM buffer (6 M guanidine hydrochloride; 0.4 M Tris-HCl, pH 8.6; 10 mM EDTA). The solution was vortexed vigorously and sonicated for 30 s under argon atmosphere. Dithiothreitol (37.5  $\mu$ L of 1 M) was added and the sample was incubated at 95°C for 10 min. Thereafter, 37.5  $\mu$ L of 1 M iodoacetamide were added and incubated for 1 h at room temperature in the dark. After each addition of chemicals, the solution was equilibrated with argon. The samples were desalted on a Smart system (Amersham Pharmacia Biotech, Freiburg, Germany) with a fast desalting column (PC 3.2/10) using 100 mM Tris-HCl with 10% acetonitrile, pH 8.5. To each sample, 2  $\mu$ g trypsin sequencing grade (Roche Diagnostics,

Mannheim, Germany) was added and incubated overnight at 37°C.

#### *Purification of glycosylated peptides by RP-HPLC*

The separation of the tryptic peptides was carried out on a Jupiter Proteo RP C12 column (4 $\mu$ , 90Å, 150  $\times$  2 mm) from Phenomenex (Aschaffenburg, Germany). The solvents were A: water with 0.1% TFA and B: acetonitrile with 0.085% TFA. For the separation, the gradient was 0–40% of B in 40 min. An aliquot of all fractions was analyzed by MALDI-TOF mass spectrometry before and after the digest with PNGaseF. One peptide with the *N*-glycosylation site 3 (amino acid residues 303–367, 6575 *m/z*) and one with the *N*-glycosylation site 1 and 2 (amino acid residues 144–200, 6241 *m/z*) were identified. The latter peptide was digested with AspN yielding two peptides (amino acid residues 152–168, 1985 *m/z* and 173–200, 2994,65 *m/z*, respectively) which were again separated by RP-HPLC.

#### *Isolation of oligosaccharides*

*N*-Glycans were cleaved from glycopeptides (for site-specific analysis) or undigested ASA (for global analysis) by PNGase F treatment. One microgram of ASA was reacted with 500 mU PNGase F (Roche Diagnostics, Mannheim, Germany) for 20 h at 37°C. Oligosaccharides were purified from the digest using carbograph solid phase extraction material (Alltech Associates, Deerfield, IL). The material was washed three times with 1 N NaOH, H<sub>2</sub>O, 70% acetonitrile with 0.1% TFA, 25% acetonitrile with 0.05% TFA, 25% acetonitrile, and water. The carbograph material was filled in a safeguard tip (Eppendorf, Hamburg, Germany) and incubated with the sample. The sample was washed with water and neutral oligoaccharides were eluted with 25% of acetonitrile. Acidic oligosaccharides were eluted with 75% acetonitrile with 0.1% TFA. Before drying the samples in a Savant SpeedVac SC100, the samples were filtered through a 0.45  $\mu$ m pipette adaptor filter (Millipore, Schwalbach, Germany).

#### *Coupling of the fluorophore*

Sixty microliters of acetic acid were mixed with 350  $\mu$ L of DMSO. In 200  $\mu$ L of this solution, 20 mg of 2-aminobenzamide was dissolved. Ten microliters of this solution was added to the dried samples (max amount 25 nmol) and incubated at 80°C for 1 h. Twelve milligrams of NaCNBH<sub>3</sub> was added and incubated at 80°C for 30 min. The sample was purified by gel chromatography on a smart system with a superdex peptide column (Amersham Pharmacia Biotech, Freiburg, Germany) at a flow rate of 50  $\mu$ L/min with water. The product and the excess of fluorophore were monitored at 320 nm.

#### *HPLC of oligosaccharide*

Oligosaccharides were separated on a TSK-gel amide-80 column (Tosoh Corporation, Tokyo, Japan). The HPLC system was from Bio-Tek (Kontron AG, Eching, Germany). The solvents were (A) acetonitrile and (B) 50 mM ammonium formate, pH 4.4. For the separation, B was increased from 30% to 50% in 75 min at a flow rate of 400  $\mu$ L/min. The column run was performed at 30°C. The fluorescence detector was a FP 2020 (Jasco, Gross-Umstadt, Germany). The wavelength for excitation was 320 nm and for emission 420 nm.

#### *Hydrolysis of dextran*

Ten milligrams of dextran (Amersham Pharmacia Biotech, Freiburg, Germany) with a molecular weight of 10,000 Da was solved in 0.5 mL 1 N acetic acid and partially hydrolyzed for 30 min at 95°C. The sample was dried and aliquots were coupled with the fluorophore 2-aminobenzamide. This partial digest was used as standard for sugar oligomers on the TSK-gel amide-80 column.

#### *Digestion of oligosaccharides with exoglycosidases*

*$\alpha$ -Fucosidase*: the dried oligosaccharides were solved in 60  $\mu$ L of 20 mM sodium acetate, pH 5.5, and 10  $\mu$ L of  $\alpha$ -L-fucosidase (Sigma-Aldrich, Munich, Germany, F 5884, bovine kidney, 1 mU/ $\mu$ L) was added. For the inhibition of the mannosidase contaminating activity, 10  $\mu$ L of D (+) mannose (18 mg/mL) was added. The sample was incubated overnight at 37°C.  *$\alpha$ -Mannosidase*: the dried oligosaccharides were solved in 76  $\mu$ L of 20 mM sodium acetate, pH 5.5, and 4  $\mu$ L of  $\alpha$ -mannosidase (Sigma-Aldrich, Munich, Germany, M7257, jack beans, 10 mU/ $\mu$ L) was added. The sample was incubated overnight at 37°C. *N-Acetylneuraminidase (sialidase)*: the dried oligosaccharides were dissolved in 25  $\mu$ L *N*-acetylneuraminidase (Roche Diagnostics, Mannheim, Germany, 1080725, vibrio cholera, 1 mU/ $\mu$ L) and incubated overnight at 37°C. *N-Acetylhexosaminidase*: the dried oligosaccharides were dissolved in 46.5  $\mu$ L of 20 mM sodium acetate, pH 5.5, and 3.5  $\mu$ L of  $\beta$ -*N*-acetylhexosaminidase (Sigma-Aldrich, Munich, Germany, A-2415, bovine kidney, 30 mU/ $\mu$ L) was added. The sample was incubated overnight at 37°C.  *$\beta$ -Galactosidase*: the dried oligosaccharides were dissolved in 4.5  $\mu$ L 50 mM sodium phosphate, pH 6.3, and 0.5  $\mu$ L of  $\beta$ -galactosidase (750 mU) was added. The sample was incubated overnight at 37°C.

#### *Global analysis of monosaccharides*

*N*-Glycans were isolated from undigested ASA polypeptides and disassembled into individual monosaccharides by 6 h boiling in 2.7 M trifluoroacetic acid. Monosaccharides including M6P residues were derivatized with anthranilic acid and separated by RP-HPLC with fluorescence detection. The peak areas were compared with peak areas from derivatized monosaccharide standards of known concentrations.

#### *MALDI-TOF mass spectrometry*

Spectra were collected with a Voyager-DE STR BioSpectrometry workstation (Applied Biosystems, Denver, CO) equipped with a 337 nm nitrogen laser. Measurements were taken manually in reflector, positive ion mode at 25 kV acceleration voltage, 68% grid voltage, and 275 ns delayed extraction time. Each mass spectrum obtained was the sum of 300 laser shots on one sample preparation.  $\alpha$ -Cyano-4-hydroxy cinnamic acid was used as a matrix (5 mg/mL in 50% acetonitrile, 0.1% TFA). One microliter of sample and 1  $\mu$ L of matrix solution were sequentially deposited on a polished stainless-steel target and crystallized at room conditions. Spectra were calibrated externally with a peptide or oligosaccharide standard, respectively. Oligosaccharides were analyzed with dihydroxybenzoic acid with 0.1% TFA in 50% acetonitrile and recrystallized with methanol.

### Determination of enzyme activity in the cell medium

$\beta$ -Hexosaminidase was determined using 10 mM par-nitrophenyl-*N*-acetyl-2- $\beta$ -D-glucosaminide, fucosidase with 10 mM 4-nitrophenyl  $\alpha$ -L-fucopyranoside, and  $\alpha$ -mannosidase with 10 mM 4-nitrophenyl  $\alpha$ -D-mannopyranoside. All substrate solutions contained 0.2% (w/v) BSA, 0.04% (w/v)  $\text{NaN}_3$ . Since we wanted to determine the activity of the enzymes at the pH in the cell medium, the substrates were not buffered. The incubation was stopped with 0.4 M glycine/NaOH, pH 10.4. The absorbance was measured at 405 nm ( $\epsilon = 18500 \text{ cm}^2/\text{mmol}$ ). For the determination of *N*-acetyl neuraminidase activity, 25  $\mu\text{L}$  of 4 mM solution of the sodium salt of 2'-(4-methylumbelliferyl)- $\alpha$ -D-*N*-acetylneuraminic acid substrate was incubated with 50  $\mu\text{L}$  of medium for 1 h. The reaction was stopped by adding 900  $\mu\text{L}$  0.2 M glycine/NaOH pH 10.4. This solution was centrifuged at  $16,000 \times g$  for 15 min. The emission of the supernatant was measured at 448 nm after excitation at 362 nm. Quantification was done with the measurement of known concentrations of 4-methylumbelliferone in a concentration range of 1 pmol/mL to 1 nmol/mL.

### Determination of mannose 6-phosphate

Since ASA contains no phosphate groups which are directly linked to the polypeptide backbone, the M6P concentration of ASA could be measured by a global analysis of its phosphate content. For this analysis, ASA was first rebuffed in 10 mM Tris/HCl pH 7.2/150 mM NaCl using a 5 mL HiTrap<sup>TM</sup> desalting column connected to an Äkta FPLC platform (GE Healthcare Europe, Munich, Germany). Then, the phosphate concentration was measured as described (Buss and Stull 1983). Briefly, 10–30  $\mu\text{g}$  of ASA was dried and ashed in the presence of magnesium nitrate to convert oligosaccharide-bound phosphate to inorganic phosphate, which could then be measured photometrically after complexation of phosphomolybdate with malachite green. As a control for a possible contamination of ASA preparations with soluble phosphates, the ashing procedure was omitted.

### Supplementary Data

Supplementary data for this article is available online at <http://glycob.oxfordjournals.org/>.

### Funding

The European Leukodystrophy Association, ELA (Q-061.0034 to U.M.).

### Abbreviations

ASA, arylsulfatase A; BHK, baby hamster kidney; CHO, Chinese hamster ovary; ERT, enzyme replacement therapy; G1, G2, G3, *N*-linked glycosylation sites of ASA at Asn158, Asn184 and Asn 350, respectively; GU, glucose units; LSD, lysosomal storage disease; M6P, mannose 6-phosphate; MLD, metachromatic leukodystrophy.

### References

Albach C, Klein RA, Schmitz B. 2001. Do rodent and human brains have different *N*-glycosylation patterns? *Biol Chem.* 382(2):187–194.

- Andersen DC, Goochee CF. 1994. The effect of cell culture conditions on oligosaccharide structures of secreted glycoproteins. *Current Opin Biotech.* 5(5):546–549.
- Arnold JN, Radcliffe CM, Wormald MR, Royle L, Harvey DJ, Crispin M, Dwek RA, Sim RB, Rudd PM. 2004. The glycosylation of human serum IgD and IgE and the accessibility of identified oligomannose structures for interaction with mannan-binding lectin I. *J Immunol.* 173(11):6831–6840.
- Beck M. 2007. New therapeutic options for lysosomal storage disorders: Enzyme replacement, small molecules and gene therapy. *Hum Genet.* 121(1):1–22.
- Bielicki J, Crawley AC, Davey RC, Varnai JC, Hopwood JJ. 1999. Advantages of using the same species for enzyme replacement therapy in a feline model of mucopolysaccharidosis VI. *J Biol Chem.* 274(51):36335–36343.
- Buss JE, Stull JT. 1983. Measurement of chemical phosphate in proteins. *Methods Enzymol.* 99, 7–14.
- Crawley AC, Brooks DA, Muller VJ, Petersen BA, Isaac EL, Bielicki J, King BM, Boulter CD, Moore AJ, Fazzalari NL, et al. 1996. Enzyme replacement therapy in a feline model of Maroteaux Lamy Syndrome. *J Clin Invest.* 97(8):1864–1873.
- Donahue RE, Wang EA, Kaufman RJ, Foutch L, Leary AC, Witel-Gianetti JS, Metzger M, Hewick RM, Steinbrink DR, Shaw G, et al. 1986. Effects of *N*-linked carbohydrates on the in vivo properties of human GM-CSF. *Cold Spring Harb Symp Quant Biol.* 51:685–692.
- Faid V, Evjen G, Tollersrud OK, Michalski JC, Morelle W. 2006. Site-specific glycosylation analysis of the bovine lysosomal alpha-mannosidase. *Glycobiology.* 16(5):440–461.
- Feizi T, Childs RA. 1987. Carbohydrates as antigenic determinants of glycoproteins. *Biochem J.* 245(1):1–11.
- Fukuda MN, Sasaki H, Lopez H, Fukuda M. 1986. Survival of recombinant erythropoetin in the circulation: The role of carbohydrates. *Blood.* 73(1):84–89.
- Gawlitzeck M, Conradt HS, Wagner R. 1995. Effect of different cell culture conditions on the polypeptide integrity and *N*-glycosylation of a recombinant model protein. *Biotechnol Bioeng.* 46(6):536–544.
- Gieselmann V, Schmidt B, von Figura K. 1992. In vitro mutagenesis of potential *N*-glycosylation sites of arylsulfatase A. Effects on glycosylation, phosphorylation, and intracellular sorting. *J Biol Chem.* 267(19):13262–13266.
- Gramer MJ, Goochee CF. 1993. Glycosidase activities in Chinese hamster ovary cell lysate and cell culture supernatant. *Biotechnol Prog.* 9(4):366–373.
- Gramer MJ, Goochee CF, Chock VY, Brousseau DT, Sliwowski MB. 1995. Removal of sialic acid from a glycoprotein in CHO cell culture supernatant by action of an extracellular CHO cell sialidase. *Biotechnology (NY).* 13(7):692–698.
- Grubb JH, Vogler C, Levy B, Galvin N, Tan Y, Sly WS. 2008. Chemically modified beta-glucuronidase crosses blood–brain barrier and clears neuronal storage in murine mucopolysaccharidosis VII. *Proc Natl Acad Sci USA.* 105(7):2616–2621.
- Guile GR, Rudd PM, Wing DR, Prime SB, Dwek RA. 1996. A rapid high-resolution high-performance liquid chromatographic method for separating glycan mixtures and analyzing oligosaccharide profiles. *Anal Biochem.* 240(2):210–226.
- Hoja-Lukowicz D, Ciolczyk D, Bergquist J, Litynska A, Laidler P. 2000. High mannose type oligosaccharides from human placental arylsulfatase A are core fucosylated as confirmed by MALDI MS. *Glycobiology.* 10(6):551–557.
- Howard DR, Natowicz M, Baenziger JU. 1982. Structural studies of the endoglycosidase H-resistant oligosaccharides present on human beta-glucuronidase. *J Biol Chem.* 257(18):10861–10868.
- Jmoudiak M, Futerman AH. 2005. Gaucher disease: Pathological mechanisms and modern management. *Br J Haematol.* 129(2):178–88.
- Kozutsumi Y, Nakao Y, Teramura T, Kawasaki T, Yamashina I, Mutsaers JH, van Halbeek H, Vliegthart JF. 1986. Structures of oligomannoside chains of alpha-mannosidase from porcine kidney. *J Biochem.* 99(4):1253–1265.
- Laidler P, Litynska A, Galka-Walczak M, Wojczyk B. 1994. Characterization of human arylsulfatase A glycans. *Int J Biochem.* 26(12):1395–1401.
- Laidler P, Litynska A. 1997. Arylsulfatase A from human placenta possesses only high mannose-type glycans. *Int J Biochem Cell Biol.* 29(3):475–483.
- Matzner U, Herbst E, Hedayati KK, Lüllmann-Rauch R, Wessig C, Schröder S, Eistrup C, Möller C, Fogh J, Gieselmann V. 2005. Enzyme replacement improves nervous system pathology and function in a mouse model for metachromatic leukodystrophy. *Hum Mol Genet.* 14(9):1139–1152.
- Matzner U, Lüllmann-Rauch R, Stroobants S, Andersson C, Weigelt C, Eistrup C, Fogh J, D'Hooge R, Gieselmann V. 2009. Enzyme replacement improves

- ataxic gait and central nervous system histopathology in a mouse model of metachromatic leukodystrophy. *Mol Ther*. 17(4):600–606.
- Miranda SR, He X, Simonaro CM, Gatt S, Dagan A, Desnick RJ, Schuchman EH. 2000. Infusion of recombinant human acid sphingomyelinase into niemann-pick disease mice leads to visceral, but not neurological, correction of the pathophysiology. *FASEB J*. 14(13):1988–1995.
- Pohl S, Marschner K, Storch S, Braulke T. 2009. Glycosylation- and phosphorylation-dependent intracellular transport of lysosomal hydrolases. *Biol Chem*. 390(7):521–527.
- Roces DP, Lüllmann-Rauch R, Peng J, Balducci C, Andersson C, Tollersrud O, Fogh J, Orlacchio A, Beccari T, Saftig P, et al. 2004. Efficacy of enzyme replacement therapy in alpha-mannosidosis mice: A preclinical animal study. *Hum Mol Genet*. 13(18):1979–1988.
- Sakuraba H, Murata-Ohsawa M, Kawashima I, Tajima Y, Kotani M, Ohshima T, Chiba Y, Takashiba M, Jigami Y, Fukushige T, et al. 2006. Comparison of the effects of agalsidase alfa and agalsidase beta on cultured human Fabry fibroblasts and Fabry mice. *J Hum Genet*. 51(3):180–188.
- Sands MS, Vogler CA, Ohlemiller KK, Roberts MS, Grubb JH, Levy B, Sly WS. 2001. Biodistribution, kinetics and efficacy of highly phosphorylated and non-phosphorylated  $\beta$ -glucuronidase in the murine model of mucopolysaccharidosis VII. *J Biol Chem*. 276(46):43160–43165.
- Schierau A, Dietz F, Lange H, Schestag F, Parastar A, Gieselmann V. 1999. Interaction of arylsulfatase A with UDP-*N*-acetylglucosamine: Lysosomal enzyme-*N*-acetylglucosamine-1-1-phosphotransferase. *J Biol Chem*. 274(6):3651–3658.
- Schmidt B, Selmer T, Ingendoh A, von Figura K. 1995. A novel amino acid modification in sulfatases that is defective in multiple sulfatase deficiency. *Cell*. 82(2):271–278.
- Sly WS. 2002. Enzyme replacement therapy: From concept to clinical practice. *Acta Paediatr Suppl*. 439:71–78.
- Staudacher E, Altmann F, Wilson IB, März L. 1999. Fucose in *N*-glycans: From plant to man. *Biochim Biophys Acta*. 1473(1):216–236.
- Storch S, Braulke T. 2005. Transport of lysosomal enzymes. In: Saftig P, editor. *Lysosomes*. Georgetown (USA): Landes Bioscience p. 17–26.
- Sun P, Sleat DE, Lecocq M, Hayman AR, Jadot M, Lobel P. 2008. Acid phosphatase 5 is responsible for removing the mannose 6-phosphate recognition marker from lysosomal proteins. *Proc Natl Acad Sci USA*. 105(43):16590–16595.
- Takahashi T, Schmidt PG, Tang J. 1983. Oligosaccharide units of lysosomal cathepsin D from porcine spleen. Amino acid sequence and carbohydrate structure of the glycopeptides. *J Biol Chem*. 258(5):2819–2830.
- Taniguchi T, Mizuochi T, Towatari T, Katunuma N, Kobata A. 1985. Structural studies on the carbohydrate moieties of rat liver cathepsins B and H. *J Biochem (Tokyo)*. 97(3):973–976.
- von Figura K, Gieselmann V, Jaeken J. 2001. Metachromatic leukodystrophy. In: Scriver CR, Beaudet AL, Sly WS, Valle D, Childs B, Kinzler KW, Vogelstein B, editors. *The Metabolic and Molecular Bases of Inherited Disease*. New York (USA): McGraw-Hill. p. 3695–3724.
- VOYNOW AA, KAISER RS, SCANLIN TF, GLICK MC. 1991. Purification and characterization of GDP-L-fucose-*N*-acetyl  $\beta$ -D-glucosaminide a 1,6 fucosyltransferase. *J Biol Chem*. 266(32):21572–21577.
- Weiss P, Ashwell G. 1989. The asialoglycoprotein receptor: Properties and modulation by ligand. *Prog Clin Biol Res*. 300:169–184.